"EXTENDED VERSION"

DYNAMIC MODELS FOR HEAT EXCHANGERS AND HEAT EXCHANGER NETWORKS

Knut W. Mathisen* , Manfred Morari,
Chemical Engineering 210-41, California Institute of Technology
Pasadena, CA 91125, USA

Sigurd Skogestad†
Chemical Engineering, University of Trondheim - NTH
N-7034 Trondheim, Norway

ABSTRACT

Dynamic models are needed to assess controllability of heat exchangers and heat exchanger networks. A simple model is desirable, but all important model features must be included. We discriminate between important and less important model features by order of magnitude argumentation, comparison of controllability measures and dynamic simulations. Important model features for single heat exchangers are number of compartments in the lumped model (model order), wall capacitance and fluid compressibility, whereas flow configuration and temperature driving force have small effect on the dynamics. Most important model features for heat exchanger networks are structure, residence time and model order of the bypasses and the connecting pipes. Simpler models may fail to identify inherent control limitations as zeros in the right half plane.

KEYWORDS

Heat exchangers; heat exchanger networks; dynamic models; lumped models; controllability

INTRODUCTION

The steady-state energy balance for heat exchangers is

$$w^h(T_i^h - T_o^h) = w^c(T_o^c - T_i^c) = UA\Delta T_{hx} \tag{1}$$

where superscript h means hot side, c cold; $w = FM_w c_p$ heat capacity flowrate and $U = h^h * h^c/(h^h + h^c)$ overall heat transfer coefficient. The overall temperature driving force of the heat exchanger, ΔT_{hx}, depends on the flow configuration. By defining the static heat exchanger effectiveness $P = (T_o^c - T_i^c)/(T_i^h - T_i^c)$ and heat capacity flow ratio $R = w^c/w^h = (T_i^h - T_o^h)/(T_o^c - T_i^c)$ the steady-state transfer function between inlet and outlet temperatures may be expressed as:

$$\begin{bmatrix} T_o^h \\ T_o^c \end{bmatrix} = \begin{bmatrix} 1-RP & RP \\ P & 1-P \end{bmatrix} \begin{bmatrix} T_i^h \\ T_i^c \end{bmatrix} \tag{2}$$

where P is a function of flow configuration, number of transfer units ($N_{TU} = (UA)/w^c$) and R only. Both P and RP are physically bounded between zero and unity, and they are usually below 0.8. R and N_{TU} are often between 0.2 and 5 except for reboilers and condensers.

We will use a dynamic model for controllability assessment, and it is known that model assumptions may be important (Hovd and Skogestad, 1991). In particular, the model must identify limitations of the achievable control performance. Important control limitations are 1) time delays, 2) right half plane (RHP) zeros, 3) input constraints and 4) sensitivity to model uncertainty. We want

*Present address: Chemical Engineering, University of Trondheim - NTH, N-7034 Trondheim, Norway
†Address correspondence to this author. Fax: 47-7-594080, E-mail: skoge@kjemi.unit.no.

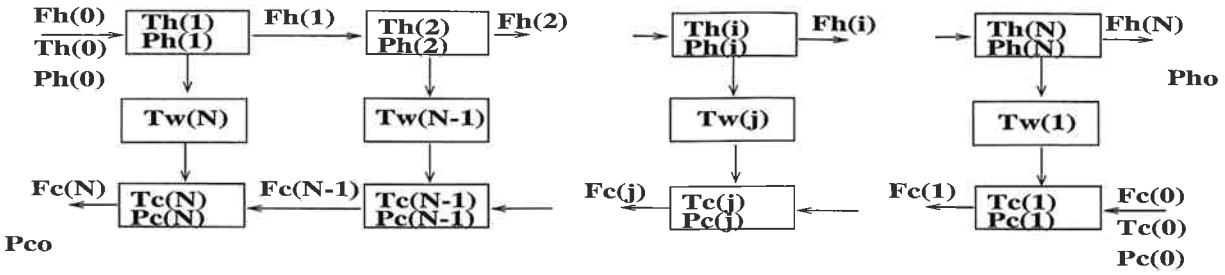

Fig. 1: Cell model of heat exchanger where fluid temperatures, wall temperatures and fluid pressures are state variables and flowrates are computed from pressure drops.

a rational transfer function and consider apparent dead-time instead of time delays. RHP zeros may occur in heat exchanger networks (HENs) that include either stream splitting or have more than minimum number of process heat exchangers. Input constraints are often a steady-state issue and will not be considered any further. HENs are not particularly sensitive to input uncertainty because elements of the relative gain array are generally below 3. Thus, we will address apparent dead-time and RHP zeros in this paper.

The following model features for single heat exchangers will be addressed: 1) heat transfer coefficients, 2) model order, 3) temperature driving force, 4) wall capacitance, 5) flow configuration and 6) fluid compressibility. For HENs we consider 1) heat transfer coefficients (again), 2) bypass placement, 3) pipe residence time, 4) model order for the pipes, 5) pressure drop and 6) actuator and sensor dynamics. We have chosen to use lumped heat exchanger models, where each fluid is modelled as mixed tanks in series, because of mathematical simplicity as well as physical resemblance to shell-and-tube exchangers with baffles. Lumped models also match experimental frequency response data well. Furthermore, when a lumped compartment or cell model is used, distributed model behaviour may be achieved by using a large number of cells or using the logarithmic mean temperature difference as the temperature driving force (Reimann, 1986; Rinard and Nieto, 1990). The latter represents a hybrid between a lumped and a distributed model. Lumped models are preferred to empirical models to get a rational transfer function and to be able to simulate different flow configurations. Furthermore, low-order heat exchanger models may become "ill-consistent" in closed-loop (Jacobsen and Skogestad, 1993). So even though both distributed models and low-order models have their advantages and may be used to study the dynamic behaviour of heat exchangers (Kawata *et al*, 1989; Ma *et al*, 1992), we will use lumped compartment or cell heat exchanger models in this paper.

The lumped compartment or "multicell model" of a heat exchanger is shown in Fig. 1. In addition to ideal mixing tank assumptions we assume negligible heat loss, constant heat capacity, and that exchanger area A and volume V are equally distributed over the N cells. For liquid exchangers fluid densities are assumed constant and pressure drop neglected. For gas exchangers densities are computed from ideal gas law and flowrates from pressure drop. For brevity, we only give the resulting differential equations for liquid exchangers including wall capacitance. A complete derivation can be found in appendix 1.

$$\frac{dT^h(i)}{dt} = (T^h(i-1) - T^h(i) - \frac{h^h A}{w^h N}\Delta T^h(i))\frac{F^h M_w^h N}{\rho^h V^h}$$

$$\frac{dT^w(j)}{dt} = (h^h \Delta T^{wh}(j) - h^c \Delta T^{wc}(j))\frac{A}{\rho^w c_p^w V^w}$$

$$\frac{dT^c(j)}{dt} = (T^c(j-1) - T^c(j) + \frac{h^c A}{w^c N}\Delta T^c(j))\frac{F^c M_w^c N}{\rho^c V^c}$$

where all symbols are explained in the nomenclature section.

The dynamic characteristics for heat exchangers are determined by flow configuration and time constants related to three holdups of energy: 1) hot side, 2) wall, 3) cold side, and may be extracted from the dynamic model as (respectively):

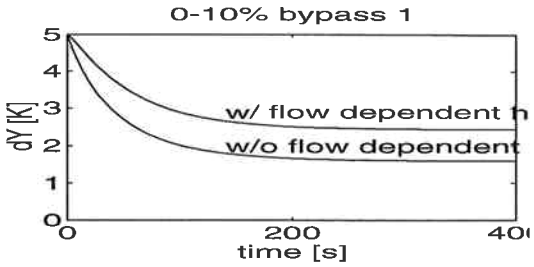

Fig. 2: Effect of flow dependent heat transfer cients. 1-1 exchanger with thermal effectiveness 0.5.

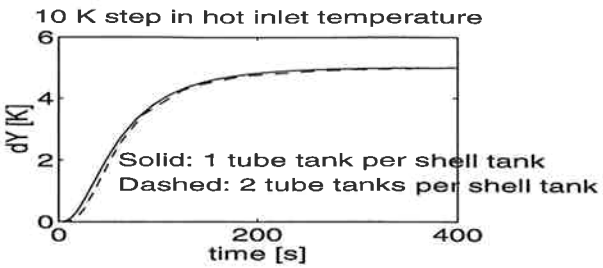

Fig. 3: Effect of 2 tube tanks per shell tank. 1-1 exchanger modelled with 6 cells with thermal effectiveness P = 0.5.

Transfer function to T_o^h from:	T_i^h	T_i^c	F^h	F^c
Lumped; h const.; w/o wall cap.; incompr.	$-N\pi/2$	$-\pi$	$-\pi/2$	$-\pi$
Lumped; h flow-dep.; w/o wall cap.; incompr.	$-N\pi/2$	$-\pi$	$-\pi/2$	$-\pi/2$
Hybrid; h const; w/o wall cap.; incompr.	$-N\pi/2$	$-\pi/2$	$-\pi/2$	$-\pi$
Hybrid; h flow-dep.; w/o wall cap.; incompr.	$-N\pi/2$	$-\pi/2$	$-\pi/2$	$-\pi/2$
Lumped; h flow-dep.; w/ wall cap.; incompr.	$-N\pi/2$	$-3\pi/2$	$-\pi/2$	$-\pi$

Table 1: Different model assumptions and model features give different asymptotic phase shifts of the frequency response.

$$\tau_F^h = \frac{V^h \rho^h}{F^h M_w^h} \qquad \tau_k^w = \frac{(V^w \rho^w c_p^w)}{(h^h + h^c)A} \qquad \tau_F^c = \frac{V^c \rho^c}{F^c M_w^c}$$

where τ_F is the residence time. Typical values are $0.5 < \tau_F < 60$ seconds and $0.1 < \tau_k = 30$ seconds. Differences in heat transfer coefficient of single- and multiphase fluids, density of gases and liquids and area density (m^2/m^3) of different heat exchangers are the main reasons for the large ranges. In most of our examples we use a liquid heat exchanger with equal heat capacity flowrates ($R = 1$) and heat transfer coefficients ($h^h = h^c$) where the time constants are $\tau_F^h = \tau_F^c = 32$ seconds and $\tau_k = 14$ seconds.

MODEL FEATURES OF SINGLE HEAT EXCHANGERS

Heat transfer coefficients

Usually heat transfer coefficients are based on a distributed heat exchanger model (i.e., U_{lm}). Heat transfer coefficients used in lumped models (U) must be increased to give the same overall effectiveness, larger increases needed for fewer cells. By combining effectiveness-expressions for one single mixing tank (Stevens *et al*, 1957) with equations for series of countercurrent heat exchangers (Domingos, 1969), the necessary heat transfer coefficient may be computed from the number of lumped cells. For equal heat capacity flowrates the relationship is simple:

$$N = \frac{N_{TU,lm}}{1 - U_{lm}/U} \qquad N_{TU,lm} = \frac{U_{lm} A}{w} \tag{3}$$

where N is the number of cells in the lumped heat exchanger model. When different model features yield different temperature driving force, we adjust heat transfer coefficients to get the same static thermal effectiveness.

From steady-state considerations the heat transfer coefficients dependence on flowrate should be included because the effects are significant. A comparison for a typical countercurrent heat exchanger ($R = 1$ and $N_{tu} = 1$) is shown in Fig. 2. Including flow dependent film coefficients will also affect dynamics by increasing the speed of response to flowrate variations. The effect is illustrated in Table 1 where the asymptotic phase shifts for different model features are compared. Note that the phase shift from cold flowrate is reduced when flow-dependent heat transfer coefficients are introduced. This makes it more desirable to include wall capacity. The table will be further commented in the following discussion of other model features.

	Min. from steady-state	Min. from dynamics	Max.
Pure lumped model	N_{TU}	2	$(N_B+1)N_P$
Hybrid model	1	3	$(N_B+1)N_P$

Table 2: Recommended number of cells. The maximum is computed from the number of baffles N_B and number of tube passes N_P, and assumes a shell-and-tube heat exchanger.

Number of mixing tanks (model order)
During simplified controllability analysis of HENs it is often implicitly or explicitly assumed a one-cell heat exchanger model (Georgiou and Floudas, 1989; Reeves it et al, 1991; Huang and Fan, 1992; Daoutidis and Kravaris, 1992). Such models will fail to predict the apparent dead-time of countercurrent heat exchangers and must be rejected from dynamic considerations. However, steady-state arguments may also be used to reject the *pure lumped* one-cell model. Consider a heat exchanger with equal heat capacity flowrates ($R = 1$) where it is assumed that the inlet temperatures are manipulated inputs (for example by manipulating bypasses of upstream heat exchangers on each stream) and the outlet temperatures are the controlled outputs. Even with infinite heat transfer coefficients, the thermal effectiveness P cannot exceed 0.5, and the transfer matrix (Eq. 1) has full rank for all parameter combinations. For two or more cells the effectiveness may become 0.5 which makes the system singular. This occurs when the outlet temperatures become equal (Reimann, 1986; Mathisen and Skogestad, 1992).

From Eq. 3 it is clear that the number of cells N must be greater than the number of transfer units N_{TU} (U will approach infinity as N approaches $N_{TU,lm}$). This simple steady-state consideration seems to be overlooked by previous authors (e.g., Papastratos *et al*, 1992). However, to be able to predict the apparent dead-time with good accuracy even more cells are usually necessary, see Fig. 4. For shell and tube heat exchangers, the number of cells is usually recommended to be one above the number of baffles (N_B), which seems intuitively attractive. It may be argued that the number of mixing tanks should be larger on the tube side than the shell side due to less back-mixing, but for typical number of cells ($N > 6$) this was found to have small effect on the apparent dead-time. A comparison for a typical countercurrent heat exchanger ($R = 1$ and $N_{tu} = 1$) is shown in Fig. 3. Furthermore, at the early design stage, discrimination between the tube and the shell side is usually not made.

Temperature driving force (hybrid or pure lumped model)
Using the logarithmic mean temperature difference (LMTD) as the temperature driving force of the cells has been suggested by several researchers (i.e., Reimann, 1986; Rinard and Nieto, 1992; Papastratos *et al*, 1992). Such a hybrid model is attractive because heat transfer coefficients are often based on a distributed model and only one cell is necessary to match any steady-state thermal effectiveness. For the hybrid model, the driving force of a mixing tank is computed from inlet temperatures as well as the tank or outlet temperatures. The response of hybrid models will therefore be faster than for pure lumped models with the same number of cells, and from dynamic considerations it may be recommended to use more cells with the hybrid model than with the pure lumped model. Our recommendations are summarized in Table 2. A comparison of the overall phase shift of the lumped and the hybrid model is given in Table 1. Note that the phase shift from cold inlet temperature and flowrate is reduced when using a hybrid model, which is a disadvantage and favors the pure lumped model compared to the hybrid model.

Because LMTD is undefined when the temperature differences on each side are equal, it may be advantageous to use Paterson-approximation of LMTD (Paterson, 1984):

$$\Delta T_{lm} \approx \frac{1}{3}(\Delta T_1 + \Delta T_2)/2 + \frac{2}{3}\sqrt{\Delta T_1 \Delta T_2}$$

where ΔT_1 and ΔT_2 are the temperature differences on each end of the exchanger. This very simple function of the arithmetric and geometric means is a good approximation of the logarithmic mean over a wide range of the two temperature differences, and it is well defined at steady-state. During a transient, however, the temperature differences may have opposite signs, and this will discontinue an on-going simulation. So for dynamic simulations, the Paterson approximation is not as helpful

as for steady-state simulation or optimization. The possibility of temperature cross-over during dynamic transients is also favors the pure lumped model compared to the hybrid model.

Wall capacitance

The time constants for energy holdup of the fluids and the wall are related:

$$\tau_k^w = \frac{(V^w \rho^w c_p^w)}{(h^h + h^c)A} = C \frac{V^w \rho^w c_p^w}{V^c \rho^c c_p^c} \frac{\tau_F^c}{N_{TU}} \qquad C\varepsilon\,[0.25, 1] \tag{4}$$

Appreciable effect of neglecting the wall capacitance is expected for large wall capacitance ratios $((V^w \rho^w c_p^w)/(V^c \rho^c c_p^c) > 1$. For liquid heat exchangers the wall capacitance ratio may well be larger than one, and this indicate that the commonly used assumption that wall capacitance may be neglected for liquid exchangers is not valid. For gas exchangers the ratio is at least an order of magnitude larger due to the lower fluid density. Thus, wall capacitance dominate the dynamics of gas exchangers, and this is in accordance with previous results. Note that the time constants for energy holdup are related through the number of transfer units N_{TU}, revealing a close connection between steady-state and dynamic behaviour of heat exchangers.

A numerical comparison with and without wall capacitance is shown in Fig. 5. The time simulation confirms that there is a considerable delay in the response when the wall capacitance is included. Additional time simulations with larger number of transfer units N_{TU} show smaller difference in the response. This is also as expected from Eq. 4 as convection becomes more important to the overall dynamics.

Flow configuration

Countercurrent 1-1 heat exchangers with one tube and one shell pass are almost invariably assumed during conceptual design. Due to mechanical, maintenance or pressure drop considerations heat exchangers with two tube passes per shell pass (1-2 exchangers) are more common in practice. Thus, we will compare dynamic behaviour of 1-1 and 1-2 exchangers, and have selected heat transfer coefficients and the number of transfer units to give the same steady-state thermal effectiveness. Interestingly, the dynamic response from 1-2 exchangers may become different from 1-1 exchangers because of the short-cut via the opposite stream, see Fig. 6, and that this appears as a dip in the phase response (Wolff *et al*, 1991). A comparison for a typical liquid exchanger is shown in Fig. 7. The temperature response for 1-1 and 1-2 exchangers with the first tube pass countercurrent is similar. The short-cut path including conduction from cold to hot and back is relatively slow, which agrees with our conclusion that wall capacitance is important for the overall dynamics. The importance of the short-cut will increase with increasing heat transfer coefficients, and will be more important for reboilers and condensers and less important for gas exchangers.

For high N_{TU} exchangers, the steady-state temperature profile of 1-2 exchangers may not be monotone due to internal temperature crossover. For illustration, consider our example exchanger with thermal effectiveness 0.6. The response to a 20% step increase in hot flowrate is inverse, see Fig. 8. This inverse response will usually not occur in practice because it requires very high number of transfer units, and it may be concluded that 1-1 and 1-2 exchangers have similar dynamics. Thus, discrimination between single and multiple tube pass exchangers is not critical for controllability assessment as long as steady-state values are accurate.

Fluid compressibility

Dynamics of gas and liquid exchanger have important differences which are mainly due to two factors concerning the density. Firstly, fluid density of gases is much lower than for liquids, which gives higher volumetric flowrates and shorter residence times. Secondly, the heat and mass balances are coupled due to the compressibility. An inlet temperature change of gas exchangers will change the flowrate, and therefore have a much faster effect on the outlet temperature on the same side than liquid exchangers. An inlet pressure change of gas exchangers will not have an immediate effect on the flow throughout the exchanger as for liquid exchangers due to the compressibility. Typical responses from gas and liquid exchangers are shown in Fig. 9. The initial response for gases are much faster than for liquids, and remain faster when heat exchangers with equal residence times are compared. The gas exchanger response is fast because the inlet temperature increase reduces the cold flowrate. The approach to steady-state is rather slow, mainly due to the considerable wall

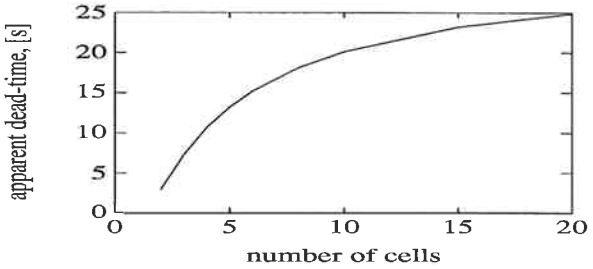

Fig. 4: Apparent dead-time from hot inlet to hot outlet temperature as function of number of cells. 1-1 exchanger without wall capacitance with thermal effectiveness P = 0.5.

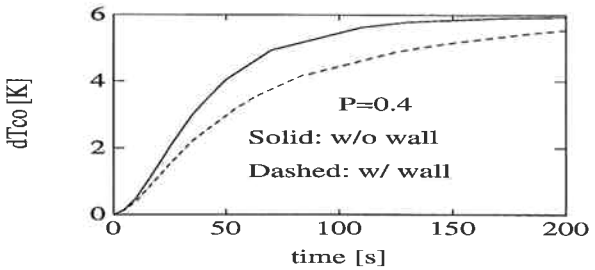

Fig. 5: Non-linear time simulation of a 1-1 heat exchanger modelled as 3 lumped cells with and without wall capacitance. Cold temperature response to 10 K hot inlet temperature increase.

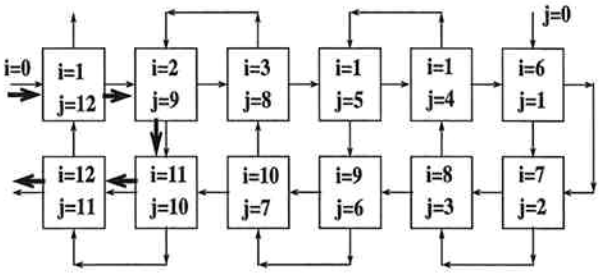

Fig. 6: Cell model of 1-2 heat exchanger showing the possible short-cut from inlet to outlet temperature of tube fluid.

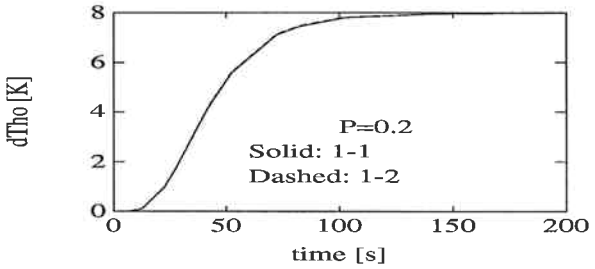

Fig. 7: Non-linear time simulation of 1-1 and 1-2 heat exchangers modelled as 12 lumped cells

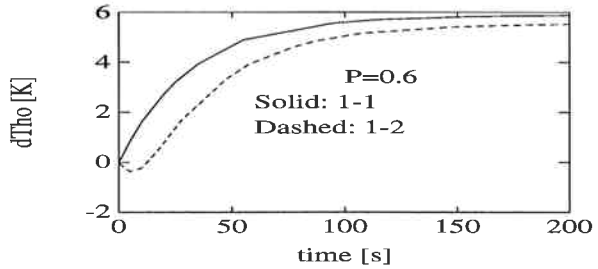

Fig. 8: Non-linear time simulation of a 1-1 and 1-2 heat exchangers modelled as 12 lumped cells. Hot temperature response to 20% hot flowrate increase.

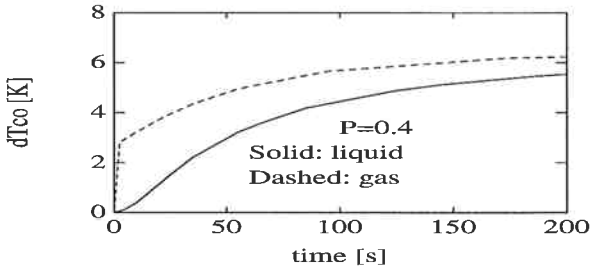

Fig. 9: Non-linear time simulation of a 1-1 liquid and gas exchangers modelled as 3 lumped cells with wall capacitance. Cold temperature response to 10 K cold inlet temperature increase.

capacitance. One may conclude that distinction between incompressible and compressible fluids is important for controllability assessment.

MODEL FEATURES OF HEAT EXCHANGER NETWORKS

In its simplest form a dynamic model of a HEN consists only of heat exchanger units and algebraic calculations for the splitter and mixers. We want to investigate the possible effect of pipe-layout, valves and measurements, too.

Heat transfer coefficients

If one fits steady-state heat transfer data as was proposed for single heat exchanger, one will have to adjust the coefficients for each exchanger separately. During conceptual design this is clearly unacceptable, one should then let the intermediate temperatures vary, and only match the outlet temperatures. Interestingly, this will tend to distribute the temperature driving forces more equally among the exchangers in the network, and thus remove a weakness of conceptual designs based on logarithmic temperature driving forces. Heggs (1985) and Kafarov *et al* (1988) have pointed out that one of the exchangers in optimized HENs often has a thermal effectiveness ($P \approx 0.9$) that is impossible to achieve using conventional shell-and-tube heat exchangers.

Bypass placement

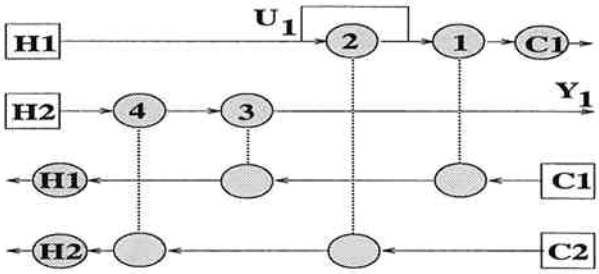

Fig. 10: Heat exchanger network where RHP-zero may exist.

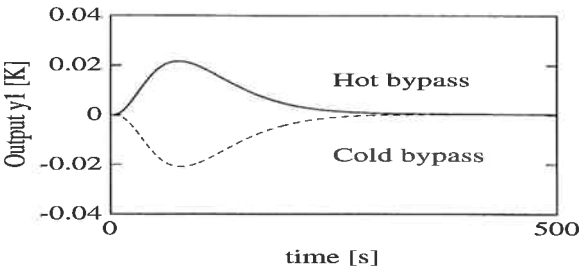

Fig. 11: Inverse response from RHP zero with bypass on hot, but not cold side of exchanger 2.

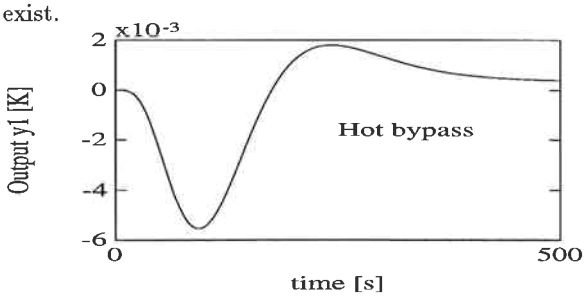

Fig. 12: Inverse response and RHP zero due to pipe residence time with bypass on cold side of exchanger 2.

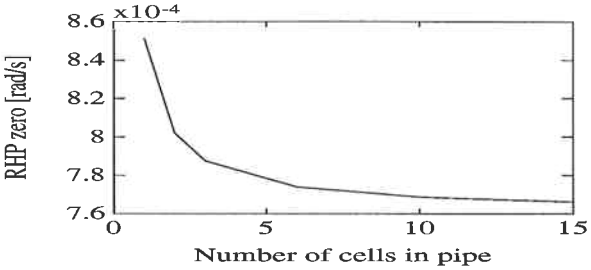

Fig. 13: RHP zero depends on pipe model order.

Bypasses are installed to be able to manipulate heat exchanger duties so that disturbances in terms of inlet temperatures and flowrates may be rejected. Clearly, around what heat exchangers the bypasses are placed is important for control. Based on steady-state considerations it does not matter whether the hot or the cold side of a given heat exchanger is bypassed, but these bypass placements are different dynamically. This difference may in some cases become very important for controllability assessment, e.g., the HEN in Fig. 10. The stream properties are equal for all the streams except for the flowrate of stream $H2$ which is 10% higher than for the other streams. The heat exchanger parameters are equal for all the exchangers, and pipe residence times are neglected. For this system, bypassing the cold side of exchanger 2 result in a system with an inverse response due to a RHP zero, whereas no such control limitation will occur if the hot side is bypassed instead, see Fig. 11. This is a somewhat extreme example, but because wall capacity is important bypass side becomes important for less extreme examples, too.

Pipe residence times

Pipe residence times should be included because they are essential for correct prediction of the apparent dead-time, and the dead-time in the pipes may exceed the dead-time in the exchangers. This will typically occur at low plant load where bypass fractions often are high. Less obvious is the fact that depending on the pipe residence time RHP zeros may or may not occur. Consider again the example in Fig. 10 and assume that the residence time in the pipe connecting exchangers 1 and 3 is of same order of magnitude as the residence times in the heat exchanger. This may give an inverse response due to a RHP zero when the hot side of exchanger 2 is bypassed, see Fig. 12.

When bypass fractions are used as manipulated inputs, it is recommended to bypass the final heat exchangers of the controlled streams to get fast responses (Mathisen *et al*, 1992). Such bypass placements make the process between manipulated inputs and controlled outputs independent of pipe residence times for incompressible fluids. However, because controllability assessment also depend on the disturbances entering at the network inlet, pipe residence times should always be included in the dynamic model of HENs.

Pipe model order

Pipe model order and pipe residence time determines the apparent dead-time in the pipes. The model order of the pipes should reflect the degree of back-mixing, and the back-mixing depends on pipe surface roughness, number and type of bends, mixing layout, valves and measurement devices. It is difficult to give general recommendations, but our experience is that three mixing tanks give a good prediction of the apparent dead-time. Sometimes the difference may be unimportant for

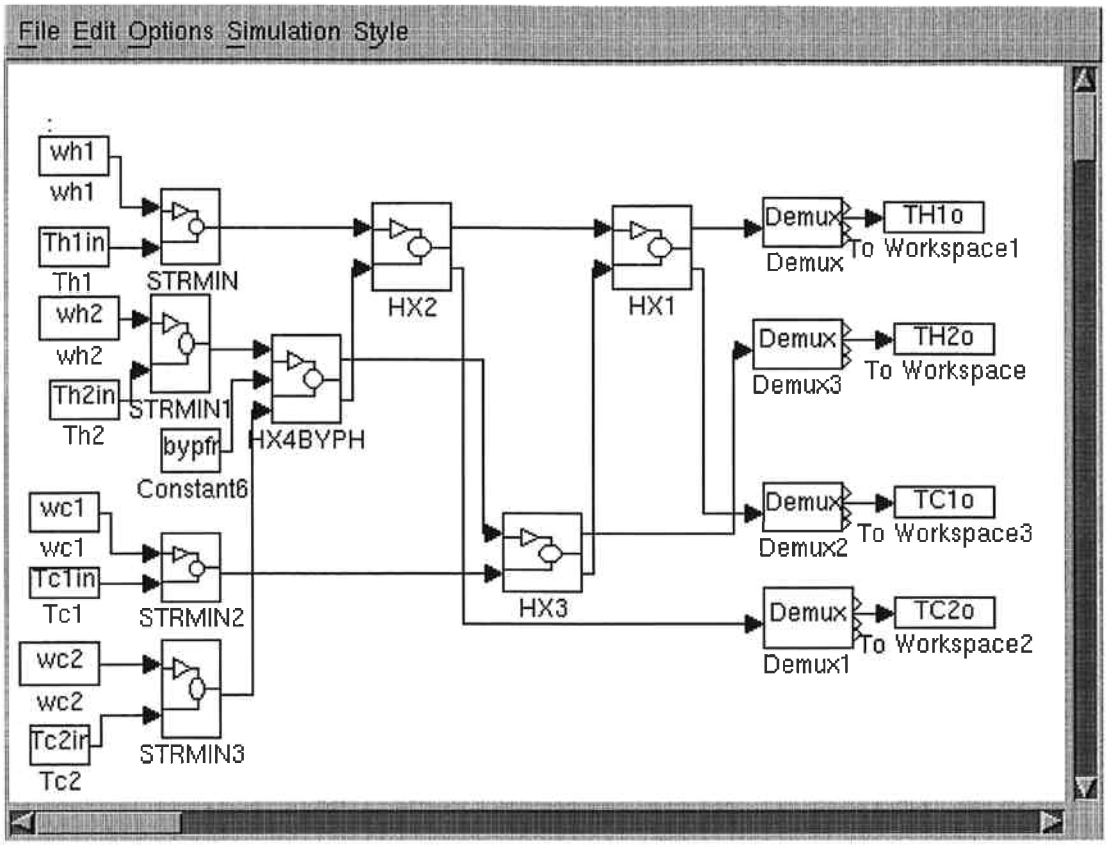

Fig. 14: SIMULINK representation of heat exchanger network.

controllability assessment. In Fig. 13 we have shown how the RHP zero of the example discussed above depends on the number of mixing tanks used to model the connecting pipe. Note that the RHP zero is just below $0.001 rad/s$ in all cases.

Pressure drop

The flowrate of gas exchangers are computed from the pressure drop. The friction factors are adjusted to match specified steady-state flowrates (in similar fashion as heat transfer coefficients are adjusted to match specified temperatures). Because pressure drops of HENs are relatively small, neither variation of the total pressure drop or the pressure drop distribution between the exchangers have appreciable effect on the dynamics.

Actuator and sensor dynamics

The dominating time constants for control valves to manipulate bypass flows and thermocouples for temperature measurements are often between 2 and 10 seconds. From comparison with time constants for energy holdup of single heat exchangers given in the introduction, it is clear that actuator and sensor dynamics may be important. The dynamic HEN model should therefore include actuator and sensor dynamics to correctly assess controllability.

EXPERIENCES WITH SIMULINK

The model was implemented in SIMULINK, a program for simulating dynamic systems with a graphic interphase (see SIMULINK User's Guide for details). A SIMULINK representation of a network with 4 streams and 4 exchangers are shown in Fig. 14. Our main reason for choosing SIMULINK was its close integration with MATLAB, which we already used for control design and analysis. Both MATLAB data and MATLAB programs may be used in the simulation, and output-data are available in the MATLAB workspace for further analysis after the simulation. SIMULINK provides a graphical interphase which enables the user to quickly and correctly set up the process flowsheet from a library of standard and user-developed moduls or *blocks*. This facility

was especially helpful for heat exchanger network applications where there are only four different process units (splitter, mixer, pipe and heat exchanger). During simulation, the integration can be followed as it proceeds through scope blocks, and parameters may be corrected without having to restart. We found these facilities helpful, and in general we have good experiences with SIMULINK. However, dynamic simulation with SIMULINK involves some disadvantages and problems, too. Some of the problems are common to sequential modular dynamic simulators; algebraic loops cannot be handled, and different boundary conditions requires different dynamic modules. With compressible fluids, the integration routines got problems with slow convergence and even numerical instability. These problems are however mainly due to the stiffness of the problem. The flow (mass) dynamics are typically several orders of magnitude faster than the temperature (energy) dynamics. A few other problems are probably due to the fact that SIMULINK was not developed with typical process engineering applications in mind. The difficulties with reusing old steady-state data for similar problems and the graphical restrictions making it impossible to draw typical countercurrent process-units were irritating and not user-friendly.

NOMENCLATURE

A	Heat exchanger area	$[m^2]$
C	Constant	$[-]$
c	Spec. heat capacity	$[J/kgK]$
D	Diameter	$[m]$
F	Molar flowrate	$[kmole/s]$
f	friction factor	$[-]$
h	Heat transfer coefficient	$[W/m^2K]$
i	Index (of tube side)	$[-]$
j	Index (of shell/wall side)	$[-]$
k	Conductance	$[W/mK]$
L	Flow trajectory array	$[-]$
M	Molar (weight)	$[kg/kmole]$
N	Number (of cells)	$[-]$
n	moles	$[kmole]$
P	Thermal effectiveness	$[-]$
P	Pressure	$[N/m^2]$
p	Prandl number exponent	$[-]$
Q	Conducted heat	$[J/s]$
q	Volumetric flowrate	$[m^3/s]$
R	Gas constant	$8314.3[J/kmoleK]$
R	Heat capacity rate ratio	$[-]$
r	Reynold number exponent	$[-]$
T	Temperature	$[K]$
t	time	$[s]$
U	Overall heat transfer coeff.	$[W/m^2K]$
U	Internal energy	$[J]$
V	Volume	$[m^3]$
v	linear velocity	$[m/s]$
w	Heat capacity flowrate	$[kW/K]$

greek

β	Volume fraction	$[-]$
ΔT	Temperature difference	$[K]$
ϵ	Roughness (of tube)	$[m]$
μ	viscosity	$[kgm/s]$
ρ	density	$[kg/m^3]$
τ	time constant	$[s]$

superscripts

c	cold side/fluid
g	gas
h	hot side/fluid
l	liquid
s	shell side/fluid
t	tube side/fluid
w	wall between fluids
0	nominal (reference)

subscripts

B	baffles
F	convection
f	flow
hx	for total exchanger
i	inlet
k	heat transfer
lm	logarithmic mean (hybrid)
o	outlet
m	main body (of exchanger)
Nu	Nusselt
P	tube passes
Pr	Prandl
p	at constant pressure
Re	Reynold
TU	transfer units
v	at constant volume
w	(molar) weight

References

[1] Correa, D.J. and J.L. Marchetti (1987). Dynamic Simulation of Shell-and-Tube Heat Exchangers. *Heat Tfr. Eng.*, 8, 50-59.

[2] Domingos, J.D. (1969). Analysis of Complex Assemblies of Heat Exchangers. *Int. J. Heat Mass Tfr.*, 12, 537-548.

[3] Heggs, P.J. (1985). Heat Exchangers for Heat Recovery. *17th Int. Symp. High Temp. Heat Exch.*, Dubrovnik, Yugoslavia.

[4] Hovd, M. and S. Skogestad (1991). Controllability Analysis for the Fluid Catalytic Cracking Process. Paper at *AIChE Ann. Mtg.*, Los Angeles, USA.

[5] Jacobsen, E.W. and S. Skogestad (1993). Inconsistencies in Dynamic Models for Ill-Conditioned Plants - with Application to Low-Order Dynamic Models of Distillation Columns. Submitted to *Chem.Eng.Sci.*

[6] Kafarov V.V., V. Zolotorev and K.N. Gureev (1988). New Approach to Synthesis of Optimal Heat-Exchanger Networks. *Doklady Akademii Nauk SSSR.*, 298, 421-424.

[7] Kawata, S., H. Kanoh and M. Masubuchi (1989). A Correlation between Steady-State and Dynamic Response of a Counterflow Heat Exchanger. *J. Dyn. Syst., Meas. Control*, 111, 115-118.

[8] Kern, D.Q., (1950). Process Heat Transfer. McGraw-Hill, Int. Ed.

[9] Ma, X.H., H.A. Preisig and R.M. Wood (1992). What determines the Accuracy of the Low-Order Models of Heat Exchangers? Paper 130b at *AIChE Ann. Mtg.*, Miami Beach, USA.

[10] Mathisen, K.W., S. Skogestad and E.A. Wolff (1992). Bypass Placement for Control of Heat Exchanger Networks. European Symposium of Computer Aided Process Engineering-1, ESCAPE-1, *Comput. Chem. Eng.*, Suppl., 17, S263-S272.

[11] Mathisen, K.W. and S. Skogestad (1992). Design, Operation and Control of Resilient Heat Exchanger Networks. Paper 141g at *AIChE Annual Mtg.*, Miami Beach, USA.

[12] Papastratos, S., A. Isambert and D. Depeyre (1993) Computerized Optimum Design and Dynamic Simulation of Heat Exchanger Networks. European Symposium of Computer Aided Process Engineering-2, ESCAPE-2, *Comput. Chem. Eng.*, Suppl., 17, S329-S334.

[13] Paterson, W.R. (1984). A Replacement for the Logarithmic Mean. *Chem. Eng. Sci.*, 39, 1635-1636.

[14] Reimann, K.A. (1986). The Consideration of Dynamics and Control in the Design of Heat Exchanger Networks. Ph.D. thesis, Univ. of Zürich, ETH, Switzerland.

[15] Rinard, I.H. and W. Nieto (1992). Heat Exchanger Modeling Considerations for Training Simulators. Paper 60a at *AIChE Spring Nat. Mtg.*, New Orleans, USA.

[16] SIMULINK User's Guide (1992). Dynamic System Simulation Software. For the X Window System. The MathWorks, Inc., Massachusetts, USA.

[17] Stevens, R.A., J. Fernandez and J.R. Woolf (1957). Mean Temperature Difference in One, Two, and Three-Pass Crossflow Heat Exchangers. *Trans. ASME*, 79, 287-297.

[18] Wolff, E.A., K.W. Mathisen and S. Skogestad (1991). Dynamics and Controllability of Heat Exchanger Networks. *Process Technol. Proc.*, 10 (Comput.-Oriented Process Eng.), 117-122.

APPENDIX 1: DYNAMIC MODEL ON STATE-SPACE FORM

Balance equations

Mole balance:

$$\dot{n}(i) = F(i-1) - F(i)$$

For incompressible fluids:

$$\dot{n}(i) = 0$$

For ideal gases:

$$\dot{n}(i) = \frac{d(P(i)V(i)/RT(i))}{dt} = \frac{V(i)}{R}\frac{d(P(i)/T(i))}{dt}$$

$$\frac{V(i)}{R}\left(\frac{1}{T(i)}\frac{dP(i)}{dt} - \frac{P(i)}{T(i)^2}\frac{dT(i)}{dt}\right) = F(i-1) - F(i) \tag{5}$$

Energy balance:

$$\dot{U}(i) = H(i-1) - H_i \pm Q_i$$

For constant specific heat capacities and reference temperature $T^0 = 0K$:

$$\dot{U}(i) = c_v V(i)\frac{d(\rho(i)T(i))}{dt} = c_p M_w(F(i-1)T(i-1) - F(i)T(i)) \pm Q(i)$$

For incompressible fluids where $c_v \approx c_p$:

$$c_p\rho(i)V(i)\frac{dT(i)}{dt} = c_p M_w F(T(i-1) - T(i)) \pm Q(i) \tag{6}$$

For ideal gases where $\rho_{=}P(i)M_w/RT(i)$ and $c_v = c_p - R/M_w$ the energy balance yields:

$$\frac{(c_p - R/M_w)V(i)}{R}\frac{dP(i)}{dt} = c_p(F(i-1)T(i-1) - F(i)T(i)) \pm Q(i) \tag{7}$$

The expression for the time derivative of the pressure ($\dot{P}(i)$) may be substituted into the mole balance:

$$\frac{V(i)}{R}\left(\frac{1}{T(i)}\frac{(c_p(F(i-1)T(i-1) - F(i)T(i)) \pm Q(i))R}{(c_p - R/M_w)V(i)} - \frac{P(i)}{T(i)^2}\frac{dT(i)}{dt}\right) = F(i-1) - F(i)$$

Gas model. The resulting equations for the fluid temperatures on state-space form become:

$$\frac{dT(i)}{dt} = ((c_p(F(i-1)T(i-1) - F(i)T(i)) - \frac{h(i) * A(i)}{M_w}\Delta T(i))/(c_v) - (F(i-1) - F(i))T(i))\frac{RT(i)}{P(i)V(i)}$$

for the wall temperatures:

$$\frac{dT^w(i)}{dt} = (h^h(i)\Delta T^{wh}(i) - h^c(i)\Delta T^{wc}(i))A(i)/(\rho_w c_p^w V(i))$$

and finally the fluid pressures:

$$\frac{dP(i)}{dt} = (c_p(F(i-1)T(i-1) - F(i)T(i)) - \frac{h(i)A(i)}{M_w}\Delta T(i))\frac{R}{V(i)(c_v)}$$

Liquid model. For liquids, we assume that the density is constant, and only temperatures are state variables. The resulting equations for the fluid temperatures on state-space form become:

$$\frac{dT(i)}{dt} = (T(i-1) - T(i) - \frac{hA(i)}{FM_w c_p}\Delta T(i))\frac{FM_w}{\rho V(i)}$$

The corresponding equations for the wall tanks are

$$\frac{dT^w(i)}{dt} = (h^h\Delta T^{wh}(i) - h^c\Delta T^{wc}(i))\frac{A(i)}{\rho^w c_p^w V^w(i)}$$

When the wall capacitance is neglected, the fluid temperatures may be calculated from:

$$\frac{dT(i)}{dt} = (T(i-1) - T(i) - \frac{UA(i)}{FM_w c_p}\Delta T(i))\frac{FM_w}{\rho V(i)}$$

Area and volume

The most important geometrical parameters are the heat transfer area A_{hx} and volume for each fluid V_{hx}^t and V_{hx}^s. For existing units, the geometrical parameters are known, or may be computed from design drawings. During design, the volume may be computed from area and volume fraction. i.e. for the shell side:

$$V_{hx}^s = \frac{A_{hx}\beta^s}{A_{spec}}$$

where the specific area per volume A_{spec} and volume fraction β^s are functions of heat exchanger type, tube diameter, tube thickness, pitch type and pitch length. For simple shell and tube heat exchanger types without fins, the specific area and volume fractions are approximately constant, and we will use the values of $A_{spec} = 80, \beta^t = 0.4, \beta^s = 0.4$ and $\beta^w = 0.2$. We assume that the area and volume of all compartments are the same, i.e. for the shell side:

$$A^s(i) = A_{hx}/N^s$$

$$V^s(i) = V_{hx}\beta^s/N^s = \frac{A_{hx}}{200N^s}$$

We further assume that the film coefficient (h) always refere to the outer heat transfer area in order to make it unnecessary to consider the surface area difference between the inside and the outside of the tubes. Area for the tube and volume for the tube and wall compartments may then be computed analogously:

$$A^t(i) = A_{hx}/N^t$$

$$V^t(i) = V_{hx}\beta^t/N^t = \frac{A_{hx}}{200N^t}$$

$$V^w(i) = V_{hx}\beta^w/N^s = \frac{A_{hx}}{400N^s}$$

Note that the number of wall compartments are equal to the number of shell compartments.

Pressure drop/flowrate

The pressure drop is usually neglected in HEN calculations, and flowrates and inlet temperatures may then be considered as disturbances. However, the reason for the flowrate disturbances are pressure variations, and for compressible fluids flowrate must be computed from the pressure drop. The pressure drop may also be used to estimate film heat transfer coefficients as in detailed heat exchanger design calculations (Jegede, 1990). The pressure drop can be calculated as:

$$\Delta P_{hx} = \Delta P_i + \Delta P_m + \Delta P_o$$

i.e., the sum of the pressure drop of the inlet or entrance region, the main body of the heat exchanger and outlet or exit region. ΔP has the form of

$$\Delta P = C\rho\frac{v^2}{2}$$

For example, the pressure drop of the main body on the tube side may be computed as

$$\Delta P_m^t = f\frac{L}{D_i^t}\rho\frac{v^2}{2} \qquad f = f(N_{Re}, \frac{\epsilon}{D^t})$$

and there are analogous, although a bit more complicated, expressions for the main part of the shell side (i.e., Kern, 1950). The pressure drop for the entrance and exit region may often be considerable compared to the pressure drop of the main body, but is highly dependent on the design. We will invariable fit pressure drop coefficients to steady-state data (assumed, estimated or measured), and assume a typical distribution of the pressure drop between the inlet, main body and outlet of the exchanger.

$$C_i = C_o = C_m/3$$

i.e., that the pressure drop of the inlet and outlet each accounts for approximately 20% of the total pressure drop. The pressure drop of the main body is distributed between the different compartments to give the following equations:

$$C(0) = C_i + C_m/2N^s = 0.20C + 0.60C/2N^s$$

$$C(i) = C_m/N^s = 0.60C/N^s; \qquad i = 1, 2, .., N^s - 1$$

$$C(N^s) = C_o + C_m/2N^s = 0.20C + 0.60C/2N^s$$

Liquids. Usually, liquids are assumed to be incompressible, so that the flow becomes constant throughout the exchanger. The molar flowrate may be computed from

$$F = \frac{A_f}{\sqrt{C_{hx}/2M_w}}\sqrt{\Delta P_{hx}\rho} \tag{8}$$

where A_f is the cross-sectional area and M_w the molecular weight

Gases. For gases, the density is computed from pressure, temperature and physical properties by a state equation. We assume the gas to be ideal and compute the density for compartment i on the tube side as $c\rho = PM_w/RT$. The pressure drop is assumed to be concentrated between the compartments, and we need the corresponding density to enter in the pressure drop equations. Pressure drop in valves are considered to depend on upstream and downstream pressures and

upstream temperature. Since, the pressure ratio (P(i)/P(i+1)) is normally close to one, we have simply used the aritmetric average of the pressures to compute the density.

$$\rho(i) = \frac{M_w}{R}\frac{P(i)+P(i+1)}{2T(i)}$$

Note that $\rho(i)$ by this convention is the density between compartment i and $i+1$. Analogically, $F(i)$ is the molar flow from compartment i and $i+1$, see Fig. 1. Substituting this equation in Eq. yields for compartment i:

$$F(i) = A_f\sqrt{\frac{1}{RM_wC(i)}}\sqrt{\frac{P(i)^2 - P(i+1)^2}{2T(i)}}$$

With constant temperature, this is the well known simplified flowrate equation for gases. Note that the pressure drop across the tank must be positive, also dynamically.

Heat conduction/Film coefficients

We compute the heat conduction to or from a fluid (Q) with a standard expression of the following form:

$$Q = hA\Delta T$$

where h is the (total) transfer coefficient, A the heat transfer area and ΔT is the temperature driving force.

The heat transfer coefficient is computed from the simple Dittus-Boelter equation:

$$N_{Nu} = CN_{Re}^r N_{Pr}^p$$

where N_{Nu} is Nusselts number hD/k; N_{Re} is Reynolds number $\rho Dv/\mu$ and N_{Pr} is Prandls number $c_p\mu/k$ and C is a constant. The exponential dependencies r and p are between 0 and 1 with typical values $0.55 < r < 0.8$ and $0.3 < p < 0.4$. When the exact exchanger type and configuration is unknown, we will normally use $r = 0.8$ as suggested by Jegede (1990) and $p = 0.33$. This yields the following expression for the film heat transfer coefficient:

$$h = CD^{r-1}\rho^r\mu^{p-r}c_p^p k^{1-p}v^r$$

For constant property fluids this may simplified to:

$$h = C'w^r \tag{9}$$

where w is the heat capacity flowrate. For ideal gases the Reynolds number can be expressed as:

$$N_{Re} = \frac{\rho Dq}{\mu A_f} = \frac{\rho DFM_w}{\mu A_f \rho} = \frac{DFM_w}{\mu A_f}$$

Since the the Reynolds number is independent of density, Eq. can be used for ideal gases as well. For our applications, the nominal film coefficients are specified rather than the constant in the Dittus-Boelter equation. The film coefficient may then be expressed as:

$$h = h^0(\frac{w}{w^0})^r$$

where h^0 is the nominal or reference film coefficient and w^0 the flowrate this coefficient referes to. We assume that wall conductance and possible resistance due to fouling are included in the film heat transfer coefficients for the fluids.

Temperature driving force

We first assume that the wall between the fluids is neglected. The driving force of a lumped parameter heat exchanger model is then simply

$$\Delta T(i) = T^t(i) - T^s(i)$$

However, we want to number the compartments on both sides in the direction of flow. Eq. is only correct for cocurrent flow. Obviously, Eq. may easily be adjusted to fit a countercurrent flow configuration for a fixed number of cells. We want to be able to handle different flow configurations and number of cells, so we have introduced tube and shell side trajectory arrays L^t and L^s. The flow trajectory arrays are defined so that $L^t(i)$ gives the mixing-tank number on the shell side that exchange heat with tube side mixing tank i. $L^s(i)$ for the shell side is defined analogously. This convenient notation is based on an idea by Correa and Marchetti (1987), but modified so that

both sides can be treated similarly. The temperature driving force for a lumped model of any heat exchanger type can then be expressed as:

$$\Delta T^t(i) = T^t(i) - T^s(L^t(i)) \qquad \Delta T^s(i) = T^s(i) - T^t(L^s(i))$$

We have derived the flow trajectory arrays as function of number of cells for some usual flow configurations. These are given in appendix 2.

More mixing-tanks on the tube side than the shell side. In practice, the degree of mixing on each side, will often be quite different. For shell and tube heat exchangers, the flow on the shell side will be considerably more backmixed than the flow in the smooth tubes. To take this difference into account, we have included a possibility to have two mixing-tanks on the tube side per mixing-tank on the shell side. The resulting flow trajectories are given in the appendix 2. The temperature driving force of the shell side must be computed as the mean of the temperatures of the corresponding mixing-tanks on the tube side. If the shell trajectory array L^s points to the final of the two tanks, the appropriate expression for the driving force is ($j = L^s(i)$):

$$\Delta T^s(i) = T^s(i) - (T^t(j) + T^t(j-1))/2$$

Logarithmic mean as the driving force. Most data for heat exchangers and heat exchanger networks are given assuming a distributed parameter model. For 1-1 countercurrent or parallel heat exchangers, the overall temperature driving force then becomes the logarithmic mean temperature difference (LMTD or ΔT_{lm}):

$$\Delta T_{lm} = \frac{\Delta T_1 - \Delta T_2}{\log(\Delta T_1 / \Delta T_2)}$$

where ΔT_1 and ΔT_2 are the temperature differences on each end of the exchanger. In order to be able to compare with other work, we have included the possibility to use LMTD in our lumped cell model. For countercurrent flow the expression for cell i on the tube side becomes

$$\Delta T_1 = T^t(i-1) - T^s(j) \qquad \Delta T_2 = T^t(i) - T^s(j-1)$$

and parallel flow

$$\Delta T_1 = T^t(i-1) - T^s(j-1) \qquad \Delta T_2 = T^t(i) - T^s(j)$$

where $j = L^t(i)$ in both cases.

Wall capacitance. The notation introduced above makes it straight forward to include wall capacitance. We assume that the mixing tanks of the wall is numbered as the mixing tanks of the shell side fluid, and the temperature driving forces for the tube and shell sides may be expressed as (assuming equal number of cells on each side):

$$\Delta T^t(i) = T^t(i) - T^w(L^t(i)) \qquad \Delta T^s(i) = T^s(i) - T^w(i)$$

whereas the driving force of the wall becomes:

$$\Delta T^{wt}(i) = T^w(i) - T^t(L^s(i)) \qquad \Delta T^{ws}(i) = T^w(i) - T^s(i)$$

when the number of mixing tanks are not equal the driving force from the wall to the tube side must be adjusted as explained above.

APPENDIX 2: FLOW TRAJECTORY

In this appendix, the flow trajectories of some common flow configurations are given. The trajectories are derived by considering one tube pass at a time. The corresponding trajectories of other configurations may be derived by using this approach, too. Note that the mathematical function $rem(i,j)$ means the remainder of the integer division i/j, e.g., $rem(1,2) = 0$ means that the integer i is even.

Equal number of mixing tanks on each side

For all these case the number of mixing tanks on the tube side is equal to the number of mixing tanks on the shell side or the wall; $N^s = N^t$. We also have that $L^t(L^s(i)) = i$ so that the shell side trajectory array is immediately known from the tube side trajectory or vice versa.

1-1 exchanger with countercurrent (C) flow. This is the default case.

$$L^t(i) = N^t - i + 1; \quad 1 \leq i \leq N^t$$

1-1 exchanger with parallel (P) flow. This case is straight forward.

$$L^t(i) = i; \quad 1 \leq i \leq N^t$$

1-2 exchanger with countercurrent-parallel (CP) flow. This case has 2 tube passes and one shell pass, and the first tube pass is countercurrent. The number of compartments must be even.

$$L^t(i) = -2i + N^t + 2; \quad 1 \leq i \leq N^t/2 \wedge rem(i,2) = 1$$

$$L^t(i) = -2i + N^t + 1; \quad 1 \leq i \leq N^t/2 \wedge rem(i,2) = 0$$

$$L^t(i) = 2i - N^t; \quad N^t/2 < i \leq N^t \wedge rem(i,2) = 1$$

$$L^t(i) = 2i - N^t - 1; \quad N^t/2 < i \leq N^t \wedge rem(i,2) = 0$$

1-2 exchanger with parallel-countercurrent (PC) flow. This case has 2 tube passes and one shell pass, and the first tube pass is parallel or cocurrent. The number of compartments must be even.

$$L^t(i) = 2i; \quad 1 \leq i \leq N^t/2 \wedge rem(i,2) = 1$$

$$L^t(i) = 2i - 1; \quad 1 \leq i \leq N^t/2 \wedge rem(i,2) = 0$$

$$L^t(i) = -2i + 2N^t + 2; \quad N^t/2 < i \leq N^t \wedge rem(i,2) = 1$$

$$L^t(i) = -2i + 2N^t + 1; \quad N^t/2 < i \leq N^t \wedge rem(i,2) = 0$$

Two tube compartments per shell compartment

One may argue that there will be less back-mixing on the tube side than the shell side. Therefore we include the flow trajectories for some common flow configurations with two mixing tanks on the tube side per mixing tank on the shell side, i.e., $N^t = 2N^s$ for all these cases. There are no restrictions on the number of cells. By definition the shell side trajectory referes to the final compartment on the tube side, so that:

$$L^t(L^s(i)) = i; \quad i = 2, 4, 6, ..N^t$$

Thus, the shell side trajectory array is known from the tube side trajectory for these cases, too.

1-1 exchanger with countercurrent (C) flow. The well-known countercurrent heat exchanger has the following trajectory.

$$L^t(i) = N^t/2 + 1 - (i+1)/2; \quad 1 \leq i \leq N^t \wedge rem(i,2) = 1$$

$$L^t(i) = N^t/2 + 1 - i/2; \quad 1 \leq i \leq N^t \wedge rem(i,2) = 0$$

1-1 exchanger with parallel (P) flow. This case is straight forward.

$$L^t(i) = (i+1)/2; \quad 1 \leq i \leq N^t \wedge rem(i,2) = 1$$

$$L^t(i) = i/2; \quad 1 \leq i \leq N^t \wedge rem(i,2) = 0$$

1-2 exchanger with countercurrent-parallel (CP) flow. This case has 2 tube passes and one shell pass, and the first tube pass is countercurrent. The number of shell side compartments must be even.

$$L^t(i) = -i + N^t/2 + 1; \quad 1 \leq i \leq N^t/2 \wedge rem(i,4) \leq 1$$

$$L^t(i) = -i + N^t/2 + 2; \quad 1 \le i \le N^t/2 \wedge rem(i,4) = 2$$

$$L^t(i) = -i + N^t/2; \quad 1 \le i \le N^t/2 \wedge rem(1,4) = 3$$

$$L^t(i) = i - N^t/2 - 1; \quad N^t/2 < i \le N^t \wedge rem(i,4) = 0$$

$$L^t(i) = i - N^t/2 + 1; \quad N^t/2 < i \le N^t \wedge rem(i,4) = 1$$

$$L^t(i) = i - N^t/2; \quad N^t/2 < i \le N^t \wedge rem(i,4) \ge 2$$

1-2 exchanger with parallel-countercurrent (PC) flow. This case has 2 tube passes and one shell pass, and the first tube pass is parallel or cocurrent. The number of shell side compartments must be even.

$$L^t(i) = i - 1; \quad 1 \le i \le N^t/2 \wedge rem(i,4) = 0$$

$$L^t(i) = i + 1; \quad 1 \le i \le N^t/2 \wedge rem(i,4) = 1$$

$$L^t(i) = i; \quad 1 \le i \le N^t/2 \wedge rem(1,4) \ge 2$$

$$L^t(i) = -i + N^t + 1; \quad N^t/2 < i \le N^t \wedge rem(i,4) \le 1$$

$$L^t(i) = -i + N^t + 2; \quad N^t/2 < i \le N^t \wedge rem(i,4) = 2$$

$$L^t(i) = -i + N^t; \quad N^t/2 < i \le N^t \wedge rem(i,4) = 3$$